

## Synthesis and Characterization of Poly(pyridine vinylene) via the Sulfinyl Precursor Route

Stijn Gillissen,<sup>†</sup> Maria Jonforsen,<sup>‡</sup> Els Kesters,<sup>†</sup> Tomas Johansson,<sup>§</sup> Mathias Theander,<sup>§</sup> Mats R. Andersson,<sup>\*,‡</sup> Olle Inganäs,<sup>§</sup> Laurence Lutsen,<sup>†</sup> and Dirk Vanderzande<sup>†</sup>

Department of Organic and Polymer Chemistry, University of Limburg, B-3590 Diepenbeek, Belgium; Polymer Technology, Chalmers University of Technology, SE-412 96 Göteborg, Sweden; and Applied Physics, Department of Physics, Linköping University, SE-581 83 Linköping, Sweden

Received April 2, 2001

**ABSTRACT:** The synthesis and characterization of poly(pyridine vinylene) (PPyV) via the nonionic sulfinyl precursor route is presented. Starting from an unsymmetrical monomer, precursor polymers were prepared in various solvents, which led to polymers with variable molecular weights. The thermal conversion to the conjugated structure, as well as its stability, was studied with different techniques such as FT-IR, UV-vis, TGA, and direct insertion probe mass spectroscopy (DIP-MS). From these results we were able to derive the most suitable conditions to perform the conversion. The fully conjugated PPyV was further characterized with photoluminescence (PL) and cyclic voltammetry (CV) measurements. The PL efficiency was found to be as high as 14%. The CV measurements showed that the polymer can be reduced (n-doped).

### Introduction

Conjugated polymers, and especially derivatives of poly(*p*-phenylene vinylene) (PPV), have been a topic of intense interest since electroluminescence was reported in this class of polymers by Burroughes et al.<sup>1</sup> Many different PPV derivatives have been synthesized in a number of ways.<sup>2</sup> Most of these polymers have low electron affinity. Conjugated polymers with high electron affinity are desired for certain applications, for example in light-emitting diodes (LEDs). High electron affinity allows the fabrication of LEDs with good electron injection from stable cathodes like aluminum rather than the low work function metals required for more electron-rich polymers.<sup>3</sup>

One way to achieve high electron affinity is to attach electron-withdrawing groups to the polymer like, for example, the cyano groups in poly[2,5-bis(hexyloxy)-1,4-phenylene-(1-cyanovinylene)] (CN-PPV).<sup>3</sup> Another way is to use electron-deficient rings in the polymer backbone.<sup>2</sup> We have used the pyridine ring, which is electron deficient due to the imine nitrogen. Poly(*p*-pyridine vinylene) was first synthesized by palladium-catalyzed cross-coupling reactions, which yielded relatively low molecular weight polymers.<sup>4</sup> The polymer obtained is insoluble in conventional organic solvents but dissolves in strong acids. It is also possible to methylate the nitrogen atom<sup>4</sup> to induce solubility in polar organic solvents. Another way to achieve a processable polymer is to synthesize a nonconjugated precursor polymer. Three different poly(*p*-pyridine vinylene) precursor polymers have been reported by Li et al.,<sup>5</sup> namely the sulfonium precursor, the chloro precursor, and the methoxy precursor. The chloro precursor route was reported to give the best results; however, it is not ideal.

The chloro precursor polymer is only soluble in strong acids like formic acid; high temperatures are needed to convert the precursor polymer to its conjugated form, and from our experience the polymerization reaction is difficult to reproduce.

In this paper we report the synthesis of poly(*p*-pyridine vinylene), starting from an unsymmetrical monomer, by the sulfinyl precursor route.<sup>6</sup> The monomer is built up of a 2,5-lutidine unit, to which a chlorine atom is attached on one side and a sulfinyl group on the other (see Scheme 1). The unsymmetrical monomer is necessary to obtain better control over the polymerization reaction and the conversion of the precursor polymer to the conjugated form by thermal elimination of the sulfinyl group.

### Experimental Section

**Materials.** All chemicals were purchased from Aldrich or Acros and used without further purification unless otherwise stated. Tetrahydrofuran (THF) was distilled over sodium/benzophenone.

**Characterization.** NMR spectra were recorded, in CDCl<sub>3</sub>, on a Varian VXR300 spectrometer. Chemical shifts ( $\delta$ ) are given in ppm relative to tetramethylsilane. The mass spectrum of the monomer was recorded on a VG ZabSpec (Fison Instruments) in positive FAB/LSIMS mode with 3-nitrobenzoyl alcohol as matrix material. The molecular weight of all precursor polymers was determined by SEC chromatography on a Waters WISP712 with three commercial Syragel columns and a Waters 410 refractive index detector. The samples were run at 30 °C with flow rate 1.0 mL/min, in chloroform, with polystyrene standards as reference.

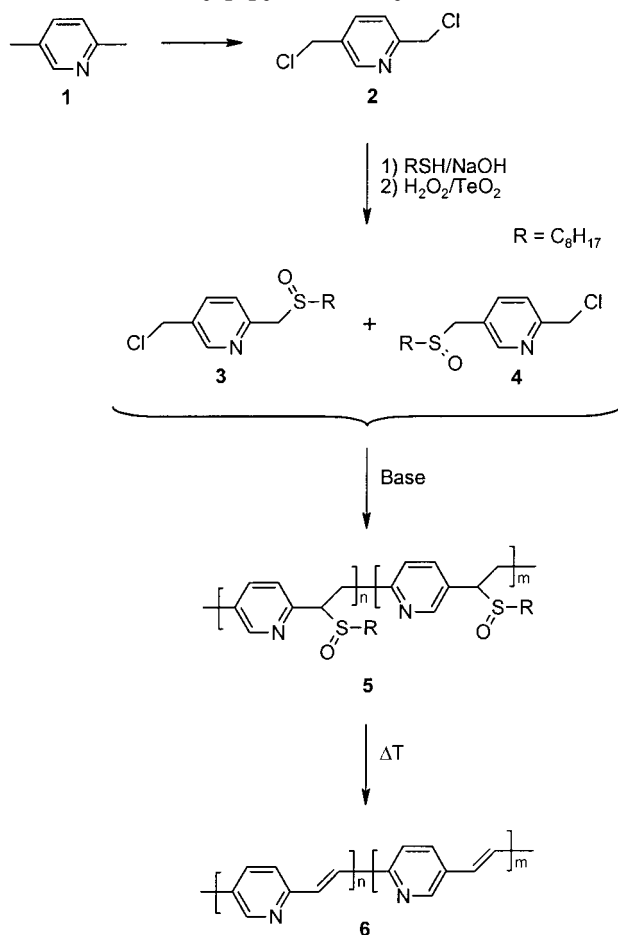
Fourier transform infrared spectroscopy (FT-IR) was performed on a Perkin-Elmer Spectrum One FT-IR spectrometer (nominal resolution 4 cm<sup>-1</sup>, summation of 16 scans). Samples for the FT-IR characterization were prepared by spin-coating precursor polymer 5 (polymerized in 50/50 vol % 2-butanol/1,4-dioxane) from a chloroform solution (6 mg/mL) onto NaCl disks (diameter 25 mm and thickness 1 mm) at 500 rpm. The NaCl disks were heated in a Harrick oven high-temperature cell (purchased from Safir), which was positioned in the beam of the FT-IR to allow in situ measurements. The temperature

<sup>†</sup> University of Limburg

<sup>‡</sup> Chalmers University of Technology.

<sup>§</sup> Linköping University.

\* Corresponding author: e-mail matsa@pol.chalmers.se; phone +46-31-772 3401; fax +34-31-772 3418.

**Scheme 1. Synthetic Pathway toward Poly(*p*-pyridine vinylene)**

of the sample and the heating source were controlled by a Watlow temperature controller (serial no. 999, dual channel). The heating source was in direct contact with the NaCl disk. Spectra were taken continuously, and the heating rate was 2 °C/min up to 450 °C. The atmosphere in the temperature cell could be varied from a continuous flow of nitrogen to vacuum (15 mmHg). Timebase software was used to investigate regions of interest.

Ultraviolet–visible spectroscopy (UV–vis) was performed on a CARY 500 UV–vis–NIR spectrophotometer (interval: 1 nm; scan rate: 600 nm/min; continuous run from 200 to 700 nm). Precursor polymer 5 (polymerized in 50/50 vol % 2-butanol/1,4-dioxane) was spin-coated from a chloroform solution (6 mg/mL) onto quartz glass (diameter 25 mm and thickness 3 mm) at 700 rpm. The quartz glass was heated in the same Harrick oven high-temperature cell as was used in the FT-IR measurements. The cell was placed in the beam of the UV–vis spectrophotometer, and spectra were taken continuously. The heating rate was 2 °C/min up to 450 °C. All measurements were performed under a continuous flow of nitrogen. Scanning kinetics software was used to investigate the regions of interest.

Thermogravimetric analysis measurements (TGA) were performed on a TA Instrument 951 thermogravimetric analyzer with a continuous nitrogen flow of 120 mL/min and a heating rate of 10 °C/min. The precursor polymer (5), polymerized in 50/50 vol % 2-butanol/1,4-dioxane, was inserted in the solid state (15 mg).

Direct insertion probe mass spectroscopy (DIP-MS) analysis of the precursor polymer was carried out on a Finnigan TSQ 70, in electron impact mode, mass range 35–650, and scan rate of 2 s. The electron energy was 70 eV. A chloroform solution of precursor polymer (5), polymerized in 50/50 vol % 2-butanol/1,4-dioxane, was placed on the heating element of

the direct insertion probe. A heating rate of 10 °C/min was used to ensure a good comparison with TGA data.

The photoluminescence (PL) spectrum of a film of the precursor polymer (5), polymerized in 50/50 vol % 2-butanol/1,4-dioxane, spin-coated from chloroform (10 mg/mL) and converted to the conjugated form by heating at 100 °C in a vacuum for 1 h, was measured by exciting the polymer sample with monochromatic light from a tungsten lamp. The emission was measured with an Oriel Intraspex IV diode matrix spectrometer. An integrated sphere made by Labsphere was used to measure the PL efficiency.<sup>7</sup>

Electrochemical measurements of the precursor polymer (5) polymerized in 50/50 vol % 2-butanol/1,4-dioxane, adsorbed on a Pt wire from a chloroform solution and converted to the conjugated form by heating at 100 °C in a vacuum for 1 h, was measured in a single-compartment electrochemical cell with a Pt counter electrode and a Ag/AgCl quasi reference electrode. Tetrabutylammonium perchlorate, 0.1 M, in acetonitrile (dried over molecular 3 Å sieves) was used as the supporting electrolyte. The cell was purged with nitrogen before each measurement. Ferrocene (half-wave potential 0.326 V vs Ag/AgCl) was used for calibration of the reference electrode.<sup>8</sup> The sweep rate was 100 mV/s unless otherwise indicated.

**Synthesis of 2,5-Bis(chloromethyl)pyridine (2).** 2,5-Lutidine (25 g, 0.23 mol) was refluxed in carbon tetrachloride (1000 mL) with *N*-chlorosuccinimide (63.7 g, 0.48 mol) and fresh benzoyl peroxide (1.0 g, 4.1 mmol) for 16 h. The solution was filtered to remove succinimide and unreacted *N*-chlorosuccinimide, washed with 10% sodium sulfite solution and water, and dried over magnesium sulfate. Thereafter, column chromatography with chloroform was used to separate the product from monochlorinated and trichlorinated compounds. After recrystallization from *n*-hexane, 9.4 g (yield 23%) of white crystals was obtained. <sup>1</sup>H NMR (CDCl<sub>3</sub>, 300 MHz): δ (ppm) 8.55 (1H, d, *J*<sub>m</sub> = 2.4 Hz); 7.77 (1H, dd, *J*<sub>m</sub> = 2.4 Hz, *J*<sub>o</sub> = 7.8 Hz); 7.47 (1H, d, *J*<sub>o</sub> = 8.1 Hz); 4.65 (2H, s); 4.57 (2H, s).

**Synthesis of Isomers 3 and 4.** Dichloride 2 (4 g, 23 mmol) dissolved in toluene (76 mL) was mixed with an aqueous solution of sodium hydroxide (4.56 g, 1.5 M) and a phase transfer reagent, Aliquat 336 (0.188 g, 6.12 mM). 1-Octanethiol (1.94 g, 13 mmol) dissolved in toluene (22 mL) was added dropwise to the mixture over 3 h. The reaction was stirred for another 17 h at room temperature. The phases were separated, and the organic layer was washed with water and dried over magnesium sulfate. After evaporation of the solvent, the crude product was dissolved in 1,4-dioxane (140 mL), and tellurium dioxide (0.53 g, 3.2 mmol) was added. Hydrogen peroxide solution (30 wt % in water, 8.61 mL) was added dropwise over 4 h. Thereafter, a few drops of concentrated hydrochloric acid were added, and the reaction was stirred for another 9 h. The reaction was quenched by adding 100 mL of brine. The solution was extracted with chloroform and dried over magnesium sulfate. Column chromatography with hexane/ethyl acetate (volume ratio 6/4) was used to separate the product from unreacted dichloride. When all dichloride had been collected, pure ethyl acetate was used to elute the product. 3.2 g (46% yield calculated from dichloride 2) of pure monomer was obtained. <sup>1</sup>H NMR showed that the product consisted of two isomers (3 and 4) in a ratio of 1:2 in favor of isomer 4. HRMS: Calcd for C<sub>15</sub>H<sub>25</sub>ClNOS: 302.135. Found: 302.139. <sup>1</sup>H NMR (CDCl<sub>3</sub>, 300 MHz): Isomer 3: δ (ppm) 8.60 (1H, d, *J*<sub>m</sub> = 2.1 Hz); 7.80 (1H, dd, *J*<sub>o</sub> = 8.1 Hz, *J*<sub>m</sub> = 2.1 Hz); 7.40 (1H, d, *J*<sub>o</sub> = 8.1 Hz); 4.59 (2H, s); 4.21 (1H, d, *J*<sub>g</sub> = 13.2 Hz); 4.08 (1H, d, *J*<sub>g</sub> = 13.2 Hz); 2.71 (1H, t, *J* = 9 Hz); 2.67 (1H, t, *J* = 9 Hz); 1.74 (2H, m); 1.40 (2H, m); 1.23 (8H, m); 0.85 (3H, t, *J* = 7.2 Hz). Isomer 4: δ (ppm) 8.48 (1H, d, *J*<sub>m</sub> = 2.1 Hz); 7.73 (1H, dd, *J*<sub>o</sub> = 8.1 Hz, *J*<sub>m</sub> = 2.2 Hz); 7.50 (1H, d, *J*<sub>o</sub> = 8.1 Hz); 4.67 (2H, s); 3.98 (1H, d, *J*<sub>g</sub> = 13.2 Hz); 3.86 (1H, d, *J*<sub>g</sub> = 13.2 Hz); 2.61 (1H, t, *J* = 9 Hz); 2.59 (1H, t, *J* = 9 Hz); 1.74 (2H, m); 1.40 (2H, m); 1.23 (8H, m); 0.85 (3H, t, *J* = 7.2 Hz). <sup>13</sup>C NMR (CDCl<sub>3</sub>, 300 MHz): Isomer 3: δ (ppm) 151.5; 149.9; 137.8; 133.3; 125.9; 59.5; 52.3; 43.3; 32.3; 29.7; 29.5; 29.4; 23.2; 23.2; 14.7. Isomer 4: δ (ppm) 157.1; 150.8; 139.4; 126.3; 123.4; 54.8; 52.0; 46.8; 32.3; 29.7; 29.5; 29.4; 23.2; 23.2; 14.7.

**Table 1. Results from Polymerization of Precursor 5 in Different Solvents**

solvent	$\bar{M}_w (\times 10^{-3})^c$	PD <sup>c</sup>	yield (%)
2-butanol <sup>a</sup>	730	5.7	50
2-butanol <sup>b</sup>	47	3.3	27
2-butanol/1,4-dioxane (50/50) <sup>a</sup>	243	4.1	52
1,4-dioxane <sup>a</sup>	17	2.1	57
THF (dry) <sup>a</sup>	56	3.2	58
DMSO <sup>a</sup>	34	2.4	17

<sup>a</sup> Base = sodium *tert*-butoxide. <sup>b</sup> Base = sodium hydroxide.<sup>c</sup> Molecular weights and polydispersities of the precursor polymer according to SEC relative to polystyrene standards with chloroform as eluent.

**Synthesis of the Precursor Polymers.** All polymers were synthesized according to the general procedure described here. Solutions of monomer (5.8 mL, 0.14 M) and base (sodium *tert*-butoxide or sodium hydroxide; 2.5 mL, 0.34 M) were prepared and degassed for 1 h by a continuous flow of nitrogen at 30 °C. The base solution was added in one portion to the stirred monomer solution. During the reaction the temperature was maintained at 30 °C, and the passing of nitrogen was continued. After 1 h the reaction mixture was poured into well-stirred ice water whereupon the polymer precipitated. The water layer was extracted with chloroform to ensure that all polymer and residual fraction were collected, and the combined organic fractions were concentrated in vacuo. The polymer was precipitated in cold ether (0 °C), collected by filtration, and dried in vacuo. The residual ether fraction was concentrated in vacuo. Polymerization results are summarized in Table 1. FT-IR: 3435 cm<sup>-1</sup> (m); 2956/2926 cm<sup>-1</sup> (s); 2856 cm<sup>-1</sup> (s); 1596/1566 cm<sup>-1</sup> (m); 1464/1484 cm<sup>-1</sup> (m); 1046/1029 cm<sup>-1</sup> (s). <sup>1</sup>H NMR (CDCl<sub>3</sub>, 300 MHz):  $\delta$  (ppm) 8.78; 8.46; 7.90; 7.68; 7.42; 7.22; 4.20; 3.74; 3.65; 2.32 (2H); 1.62 (2H); 1.20 (10H); 0.84 (3H). <sup>13</sup>C NMR (CDCl<sub>3</sub>, 300 MHz):  $\delta$  (ppm) 157.2; 151.6; 150.6; 150.1; 137.3; 136.2; 133.4; 132.8; 124.3; 69.8; 66.4; 48.3; 31.6; 29.0; 28.8; 28.7; 22.5; 13.9.

## Results and Discussion

**Monomer Synthesis.** The monomer synthesis (see Scheme 1) started from the commercially available 2,5-lutidine, which was chlorinated with *N*-chlorosuccinimide.<sup>9</sup> Dichloride **2** is unstable at room temperature and decomposes spontaneously to an unknown red substance; however, it can be stored at -25 °C for longer periods without degrading. The thioether group is introduced in a two-phase reaction using 1-octanethiol, sodium hydroxide, and a phase transfer reagent, Aliquat 336.<sup>10,11</sup> We used 1-octanethiol because the long aliphatic chain guarantees good solubility of both monomer and precursor polymer. Because of the asymmetric position of the chloromethyl substituents on the pyridine ring, we ended up with a mixture of two isomers in this reaction. After oxidation of the crude product, to the sulfoxide, using H<sub>2</sub>O<sub>2</sub>/TeO<sub>2</sub> in 1,4-dioxane,<sup>12</sup> the ratio between the two isomers was determined by <sup>1</sup>H NMR experiments and found to be 2:1 in favor of the 5-substituted isomer **4**. The isomers were inseparable using simple chromatographic or crystallization techniques. As a consequence, the mixture of isomers was used in all polymerization reactions.

**Synthesis of the Precursor Polymer.** All polymerizations were carried out under the same conditions (see Experimental Section) in a range of solvents and solvent mixtures (see Table 1). We chose to use the base sodium *tert*-butoxide, which was added in solution in a slight excess of 1.05 equiv to correct for losses during addition. The polymerization time was 1 h, after which the reaction mixture was poured into water. The polymer was extracted with chloroform, concentrated, and pre-

cipitated in diethyl ether. The precursor polymers and the residual fractions were analyzed. The precursor polymers were soluble in organic solvents such as chloroform and THF as well as in formic acid.

The precursor polymer was obtained in all tested solvents (see Table 1). The highest yields were obtained in aprotic solvents like THF and 1,4-dioxane, whereas the highest molecular weight was found in the protic "less polar" solvent 2-butanol. When the polymerization was performed in a 50/50 (vol %) mixture of 2-butanol and 1,4-dioxane, an intermediate molecular weight and polymerization yield were obtained. A possible explanation to this was found when analyzing the residual fraction with <sup>1</sup>H NMR. The residual fraction from the polymerization in the 50/50 mixture of 2-butanol and 1,4-dioxane contained a fraction of monomer that had been solvent substituted; i.e., 2-butoxide had replaced the chlorine group. In pure 2-butanol the residual fraction consisted only of solvent-substituted monomer, while with pure 1,4-dioxane or THF the residual fraction consisted only of unreacted monomer. This side reaction may account for the lower polymerization yield in 2-butanol. We have seen that, for PPV, solvent substitution in 2-butanol can be avoided by changing the base to sodium hydroxide without affecting the outcome of the polymerization.<sup>13</sup> This is true for PPV, but in the case of PPV, both polymerization yield and molecular weight drop significantly yet solvent substitution is still observed.

When the polymerization was performed in a polar aprotic solvent like DMSO, premature elimination of the sulfinyl group in the precursor polymer occurred. This resulted in an insoluble conjugated fraction, which could not be analyzed. A small fraction of soluble precursor polymer was formed, but due to the side reaction the yield was rather low.

From these results we can conclude that we have some control over the molecular weight of the polymer by using different solvents or solvent mixtures. In the following experiments we have used precursor polymer synthesized in a 50/50 (vol %) mixture of 2-butanol and 1,4-dioxane.

**Conversion to, and Thermal Stability of, the Conjugated Structure.** The final step in the sulfinyl precursor route is thermal elimination of the sulfinyl group to give the double bond. The process by which the sulfinyl groups are eliminated is an expulsion of sulfenic acid and formation of a double bond on the polymer backbone.<sup>14</sup> The double bond formed is mainly trans due to steric hindrance in the transition state. The sulfenic acids which are split off are unstable and dimerize immediately to give thiosulfonates and water. The thiosulfonates disproportionate to thiosulfonates and disulfides.<sup>15,16</sup> Numerous techniques can be applied to monitor the elimination process. The ones used here are FT-IR, UV-vis, TGA, and direct insertion probe mass spectroscopy (DIP-MS).

FT-IR spectroscopy measurements were carried out on film, spin-coated on NaCl disks. An experimental setup was used (see Experimental Section) which allowed in situ monitoring of the elimination process. A dynamic heating program of 2 °C/min up to 450 °C, under a continuous flow of nitrogen, was used. The most distinct absorption bands, which are changed during the elimination process, are the sulfoxide band at 1040 cm<sup>-1</sup> and the trans vinylene band at 960 cm<sup>-1</sup>. The elimination and the degradation process can be followed from



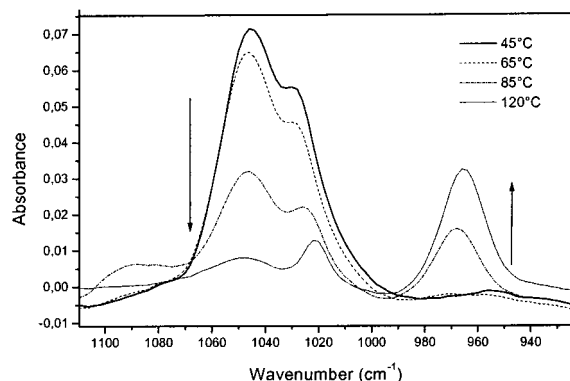


**Figure 1.** Enlarged part of the IR spectrum showing sulfoxide and vinylene absorption bands.

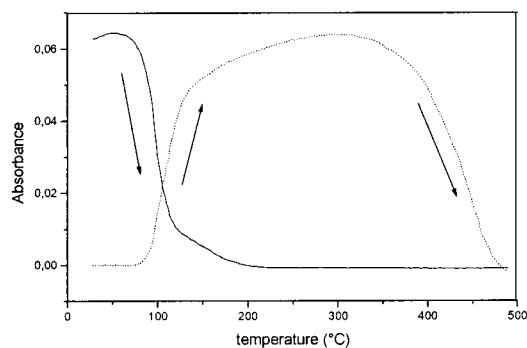


**Figure 2.** Sulfoxide (1040  $\text{cm}^{-1}$ , solid line) and vinylene (960  $\text{cm}^{-1}$ , dotted line) absorption vs temperature.

the intensity of the vinylene signal at 960  $\text{cm}^{-1}$ . Figure 1 shows an enlarged part of the IR spectrum at a few selected temperatures. We clearly observe the relative trends in elimination behavior. The sulfoxide absorption declines as the double-bond absorption appears. In Figure 2, the sulfoxide (1040  $\text{cm}^{-1}$ ) and double-bond (960  $\text{cm}^{-1}$ ) absorption are plotted vs increasing temperature. Both elimination and double-bond formation start around 75 °C, and when the temperature reaches 130 °C, the processes slow down considerably, with hardly any change seen after 200 °C. When even higher temperatures are reached, a decline in double-bond signal is observed. This decomposition of double bonds starts at approximately 310 °C and ends at 450 °C when almost no double-bond signal remains. Both formation and decomposition of the vinylene double bond are shown in Figure 2. Changing the atmosphere from a continuous flow of nitrogen to vacuum (15 mmHg) gave a curve that was similar to the one shown in Figure 2, but the maximal double bond absorption was reached at 140 °C compared to 310 °C in nitrogen. These results suggest that the elimination in nitrogen atmosphere takes place between 90 and 310 °C. By applying vacuum, elimination and evaporation of elimination products are complete at 140 °C.

UV-vis spectroscopy measurements were carried out on film, spin-coated on quartz. The heating setup was the same as in the IR experiments, and a dynamic heating program of 2 °C/min up to 450 °C under a continuous flow of nitrogen was used. Before heating, two absorption bands from the precursor polymer were present (maxima at 218 and 273 nm). As the heating program progressed, new absorption bands appeared that gradually red-shifted with increasing temperature. When higher temperatures were reached, the fine

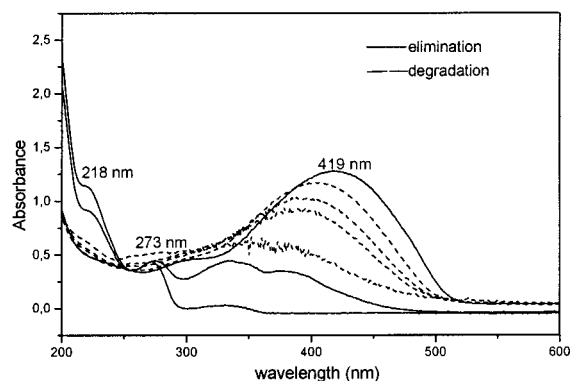


**Figure 3.** UV-vis spectra of the formation (30, 98, 130 °C; solid lines) and degradation (340, 360, 390, 430 °C; dashed lines) of the conjugated structure.

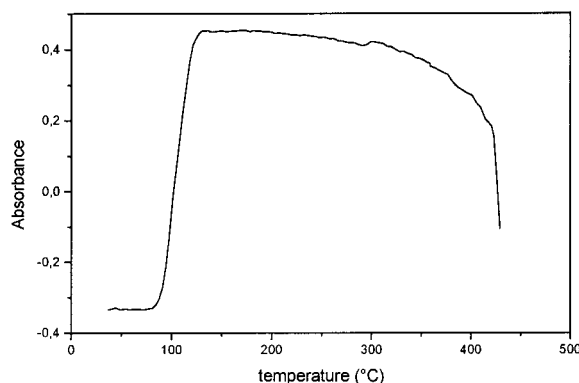


**Figure 4.** Absorption at 419 nm vs temperature.

structure disappeared and the absorption band broadened to cover the various oligomer bands. When, at 130 °C, the absorption was maximal, a conjugated polymer with an absorption maximum around 419 nm was obtained. The gradual formation of the conjugated structure is shown in Figure 3 (solid lines). At higher temperatures the absorbance declined very slowly until 310 °C. The decay was very small and is probably due to thermochromism rather than degradation, which means that the polymer was stable up to 310 °C. At 310 °C the absorbance at 419 nm started to decline faster. Together with this decline, a blue shift in absorption maximum was noticed which may be explained by a shortening of the conjugated segments. When 450 °C was reached, the absorbance was more than halved, and a very broad signal remained. The gradual decomposition of the conjugated structure is also shown in Figure 3 (dashed lines). When the absorbance at 419 nm is plotted vs temperature (Figure 4), we conclude that the conjugated structure is formed between 75 and 130 °C and degradation occurs between 310 and 450 °C. This result is in accordance with the FT-IR results.

The TGA experiment was performed in nitrogen atmosphere. The thermogram shows several steps of weight loss. Two major steps of weight loss are visible. The first one (120–310 °C) is due to the elimination of the sulfoxide groups and evaporation of elimination products. The second period of weight loss (450–550 °C) accounts for the degradation of the polymer backbone. After elimination, at 310 °C, an experimental residual weight of approximately 40% remains. This is in accordance with the theoretical residual value (39%). A typical thermogram is shown in Figure 5. The temperature observed with TGA was slightly different than

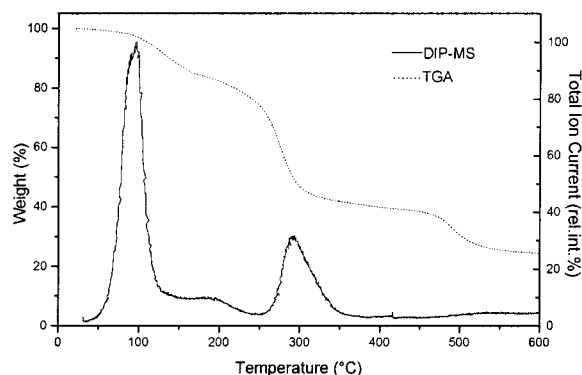


**Figure 5.** TGA thermogram (dotted line) and DIP-MS thermogram (solid line) of the precursor polymer.

**Table 2. DIP-MS Results: Mass Fragments of the Elimination Products**

<i>m/z</i>	fragment	rel int (%)
307	$[\text{C}_8\text{H}_{17}\text{S}(\text{O})\text{SC}_8\text{H}_{17}]^+$	4
289	$[\text{C}_8\text{H}_{17}\text{SSC}_8\text{H}_{17}]^+$	10
194	$[\text{SS}(\text{O})\text{C}_8\text{H}_{17}]^+$	10
161	$[\text{S}(\text{O})\text{C}_8\text{H}_{17}]^+$	100
145	$[\text{SC}_8\text{H}_{17}]^+$	35
71	$[\text{OC}_4\text{H}_7]^+$	70
63	$[\text{CH}_3\text{SO}]^+$	20
57	$[\text{C}_4\text{H}_9]^+$	90
43	$[\text{C}_3\text{H}_7]^+$	50

that observed with FT-IR and UV-vis measurements, probably because of a thicker sample which prevents evaporation of the elimination products in the TGA. The faster heating in the TGA experiment can also contribute to the rise in the observed elimination temperature.

The elimination was also studied by DIP-MS, to allow the analysis of the elimination products. In this technique the precursor polymer is placed directly on the heating element of the probe. By plotting the total ion current vs temperature, the thermal stability of both precursor and conjugated polymer can be visualized. In accordance with the TGA measurements two signals were observed which can be assigned to an elimination step (80–110 °C) and a degradation step (270–320 °C) (see Figure 5). The decrease in elimination and degradation temperature compared to the case of TGA is caused by the high vacuum ( $10^{-6}$  mmHg) at the probe which makes the elimination products evaporate faster. In TGA continuous nitrogen flow is used. The fragments analyzed by MS correspond to the ones of the expected elimination products<sup>16</sup> (see Table 2).

To conclude, the difference in elimination temperature observed with the different techniques suggests that, under nitrogen atmosphere, elimination is complete at 130 °C, but elimination products stay in the film until 310 °C. To get a better evaporation of elimination products, the pressure can be reduced. This means that elimination, for thin samples, is best conducted at a temperature between 100 and 130 °C to prevent degradation of the polymer but still get good conversion. Furthermore, it is advisable to apply vacuum during the conversion to get complete evaporation of the elimination products. Without reducing the pressure, heating to 200–250 °C is necessary to get complete elimination and evaporation of elimination products. The different spectroscopic data suggest that degradation starts at about 270 °C; therefore, higher temperatures should not be used during conversion. We chose to use 100 °C in vacuum for 1 h for the preparation of the films used in our analysis of PPyV.

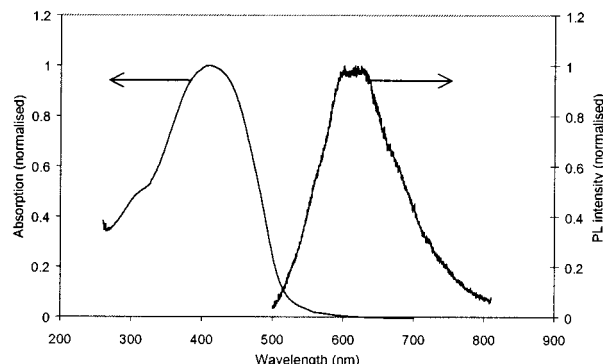


**Figure 6.** Absorption and photoluminescence spectra for PPyV.

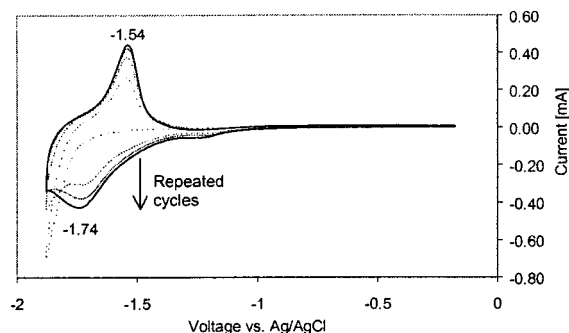


**Figure 7.** Cyclic voltammogram of PPyV.

**Absorption and Photoluminescence.** The photoluminescence (PL) and absorption spectra of a PPyV film that has been converted to its conjugated form by heating at 100 °C in a vacuum for 1 h are shown in Figure 6. The maximum photoluminescence intensity is at about 600 nm. The PL efficiency measured with an integrated sphere was 14%. This is a much higher value than those previously reported for PPyV (1.5–2%).<sup>5,17</sup> A likely explanation for the higher efficiency for our film is a different morphology. This can be caused by a difference in molecular weight, the long alkyl groups in our precursor polymer, or spin-coating from chloroform rather than formic acid. The thermal conversion from precursor polymer to the conjugated form can also affect the morphology. Since our polymer has higher PL efficiency than both PPyV polymerized by stepwise polymerization<sup>17</sup> and PPyV synthesized via the chloro precursor,<sup>5</sup> it is probably not the molecular weight or the thermal treatment alone that causes the difference. More experiments are needed to test these hypotheses.

**Electrochemical Properties.** A cyclic voltammogram of a PPyV film on a Pt electrode is shown in Figure 7. No reduction is seen during the first cycle, probably because the film is very compact and has to be swelled first. In the second scan, a peak has started to form, and in the third and fourth scans it is seen clearly, with the reduction peak at -1.74 V vs Ag/AgCl. The corresponding oxidation (n-undoping) is at -1.54 V vs Ag/AgCl. The reduction of the polymer is reversible, but the oxidation of PPyV is irreversible with a peak at 1.2 V vs Ag/AgCl (sweep rate 10 mV/s, not shown). The band gap calculated from the formal reduction potential (estimated as the average of the reduction and reoxidation peaks to be -1.64 V vs Ag/AgCl) and the oxidation peak is 2.84 eV, which is in accordance with the UV maximum (about 2.9 eV). For comparison, PPV, synthesized via the octylsulfanyl precursor<sup>18</sup> and con-

verted to the conjugated form at 120 °C for 1 h at reduced pressure, and CN-MEH-PPV, synthesized as described in the literature,<sup>2</sup> were measured under the same conditions as PPyV. PPV had a formal potential of  $-2.03$  V vs Ag/AgCl and CN-MEH-PPV  $-1.30$  V vs Ag/AgCl, which is similar to previously reported values.<sup>19</sup> This means that our polymer has lower electron affinity than CN-MEH-PPV but much higher than PPV.

### Conclusions

We have prepared poly(*p*-pyridine vinylene) starting from an unsymmetrical monomer, built up of 2,5-lutidine with a chlorine group attached on one side and a sulfinyl group on the other. This gave good control over the polymerization process. By using different solvents, precursor polymers with different molecular weights are obtained. This means that we have a way of controlling the molecular weight. When the conversion of the precursor polymer to the conjugated form was studied, it was seen that for thin films the conversion is best performed either in a vacuum at 100–130 °C or in nitrogen at 200–250 °C. PPyV is stable up to at least 270 °C under these conditions. The PL efficiency for PPyV converted to the conjugated form in a vacuum, as described above, was 14%. This is much higher than previously reported for PPyV, probably due to different morphology. CV measurements showed a reversible reduction, with formal potential  $-1.64$  V vs Ag/AgCl, and an irreversible oxidation.

**Acknowledgment.** Financial support for this work has been provided by the Swedish Foundation for Strategic Research, Ericsson's Research Foundation, and the Flemish institute for promotion of the scientific technological research in the industry (IWT). We also thank M. Björklund and J. Linnér for help with the SEC measurements, G. Stenhagen with the mass spectra of the monomers, J. Czech for the DIP-MS measurements, G. Reggers for the TGA measurements, and Mikael Johansson for the synthesis of CN-MEH-PPV.

### References and Notes

- (1) Burroughes, J. H.; Bradley, D. D. C.; Brown, A. R.; Marks, R. N.; Mackay, K.; Friend, R. H.; Burns, P. L.; Holmes, A. B. *Nature* **1990**, *347*, 539.
- (2) Kraft, A.; Grimsdale, A. C.; Holmes, A. B. *Angew. Chem., Int. Ed.* **1998**, *37*, 402–428.
- (3) Greenham, N. C.; Moratti, S. C.; Bradley, D. D. C.; Friend, R. H.; Holmes, A. B. *Nature* **1993**, *365*, 628–630.
- (4) Marsella, M. J.; Fu, D. K.; Swager, T. M. *Adv. Mater.* **1995**, *7*, 145–147.
- (5) Li, X.-C.; Cacialli, F.; Cervini, R.; Holmes, A. B.; Moratti, S. C.; Grimsdale, A. C.; Friend, R. H. *Synth. Met.* **1997**, *84*, 159–160.
- (6) Louwet, F.; Vanderzande, D.; Gelan, J.; Mullens, J. *Macromolecules* **1995**, *28*, 1330–1331.
- (7) Theander, M.; Mammo, W.; Olinga, T.; Svensson, M.; Andersson, M. R.; Inganäs, O. *J. Phys. Chem. B* **1999**, *103*, 7771–7780.
- (8) Bard, A. J.; Faulkner, L. R. *Electrochemical Methods, Fundamentals and Applications*; John Wiley & Sons: New York, 1980; pp 701–702.
- (9) Klemm, L. H.; Johnson, W. O.; White, D. V. *J. Mater. Chem.* **1972**, *9*, 843–848.
- (10) Herriott, A. W.; Picker, D. *Synthesis* **1975**, 447–448.
- (11) Issaris, A.; Vanderzande, D.; Adriaenssens, P.; Gelan, J. *Macromolecules* **1998**, *31*, 4426–4431.
- (12) Kim, K. S.; Hwang, H. J.; Cheong, C. S.; Hahn, C. S. *Tetrahedron Lett.* **1990**, *31*, 2893–2894.
- (13) van Breemen, A.; Issaris, A. C. J.; de Kok, M. M.; Van der Borgh, M.; Adriaenssens, P. J.; Gelan, J.; Vanderzande, D. J. M. *Macromolecules* **1999**, *32*, 5728–5735.
- (14) Kingsbury, C. A.; Cram, D. J. *J. Am. Chem. Soc.* **1960**, *82*, 1810–1819.
- (15) Davis, F. A.; Jenkins, L. A.; Billmers, R. L. *J. Org. Chem.* **1986**, *51*, 1033–1040.
- (16) de Kok, M. M.; van Breemen, A.; Carleer, R. A. A.; Adriaenssens, P. J.; Gelan, J. M.; Vanderzande, D. J. *Acta Polym.* **1999**, *50*, 28–34.
- (17) Blatchford, J. W.; Jessen, S. W.; Lin, L. B.; Gustafson, T. L.; Fu, D. K.; Wang, H. L.; Swager, T. M.; MacDiarmid, A. G.; et al. *Phys. Rev. B: Condens. Matter* **1996**, *54*, 9180–9189.
- (18) Issaris, A.; Vanderzande, D.; Gelan, J. *Polymer* **1997**, *38*, 2571–2574.
- (19) Li, Y.; Cao, Y.; Gao, J.; Wang, D.; Yu, G.; Heeger, A. J. *Synth. Met.* **1999**, *99*, 243–248.

MA010575W